Phytopathology Research

RESEARCH

Open Access

Crystal structure of rice APIP6 reveals a new dimerization mode of RING-type E3 ligases that facilities the construction of its working model

Yangyang Zheng[1], Xin Zhang[1], Yang Liu[1], Tongtong Zhu[1], Xuefeng Wu[1], Yuese Ning[2], Junfeng Liu[1,3] and Dongli Wang[1*]

Abstract

Ubiquitination is an important modification process in eukaryotic organisms, and ubiquitin ligase (E3) is the most diversified component of this system. APIP6 (AvrPiz-t interacting protein 6) is one of the E3s of rice, and is involved in the recognition of AvrPiz-t, one effector from the pathogen *Magnaporthe oryzae*, for the initiation of host defense against *M. oryzae*. However, the structural detail of how APIP6 performs its function remains elusive. Here, we present crystal structure of the RING domain (i.e., the E2-interaction domain) of APIP6 (APIP6-RING). APIP6-RING exists as a homodimer in crystal packing, in solution and in vivo. APIP6-RING consists of one β hairpin and one α helix, and β hairpins of two APIP6-RING molecules interact with each other in a novel 'shoulder-to-shoulder' mode to form a β sheet, and also rendering APIP6-RING to form a homodimer. Hydrogen bonds play a major role in the dimer formation of APIP6-RING, while hydrophobic-intermolecular interactions are inconspicuous. Due to the interaction mode between RING-type E3 and E2 is generally conserved, we constructed and verified a model of APIP6-RING/E2 complex, and proposed a working model of APIP6 with E2, ubiquitin, and the substrate AvrPiz-t. Taken together, our research presents the first structure of plant simple RING-type E3 ligase that exists in an unreported dimerization manner, as well as a working model of APIP6.

Keywords Rice, *Magnaporthe oryzae*, Ubiquitination, E3 ligase, APIP6, RING, Crystal structure

Background

Ubiquitination is one of the post-translational modifications of eukaryotic cells that regulate various processes, such as protein degradation and signaling (Buetow and Huang 2016). Ubiquitination typically involves five components: ubiquitin (Ub), ubiquitin-activating enzyme (E1), ubiquitin conjugating enzyme (E2), ubiquitin ligase (E3), and substrate (Buetow and Huang 2016). Ubiquitin is a conserved protein of 76 amino acids with a canonical ubiquitin fold (Vijaykumar et al. 1987). With the help of ATP and a magnesium ion, E1 activates ubiquitin by forming a thioester bond between its catalytic cysteine and the di-glycine motif at the C-terminal of ubiquitin,

*Correspondence:
Dongli Wang
wdl@cau.edu.cn
[1] Ministry of Agriculture Key Laboratory for Crop Pest Monitoring and Green Control, College of Plant Protection, China Agricultural University, Beijing 100193, China
[2] State Key Laboratory for Biology of Plant Diseases and Insect Pests, Institute of Plant Protection, Chinese Academy of Agricultural Sciences, Beijing 100193, China
[3] Joint International Research Laboratory of Crop Molecular Breeding, China Agricultural University, Beijing 100193, China

and then transfers the thioester bond to the catalytic cysteine of E2 (Pruneda et al. 2012; Soss et al. 2013; Buetow and Huang 2016). The E2/Ub complex is flexible until the participation of E3, which stabilizes the overall conformation of the E2/Ub complex and recruits substrate to initiate ubiquitination (Pruneda et al. 2012; Soss et al. 2013; Buetow and Huang 2016). There are three types of E3s: RING (really interesting new gene) E3s, HECT (homologous to E6AP C-terminus) E3s, and RBR (RING-between-RING) E3s (Morreale and Walden 2016). E1 and E2 are generally conserved, while due to bearing the vital role of substrate selection, E3 is highly diverse, especially in plants. For example, in the genome of cultivated rice (*Oryzae sativa* L.), around 1513 E3s were identified (Wang et al. 2022).

Plants mainly use cytosolic nucleotide-binding leucine-rich repeat receptors (NLRs) to recognize effectors of pathogens and then initiate immune responses (Ngou et al. 2022). Rice production is threatened by the devastating blast disease caused by the pathogenic fungus *Magnaporthe oryzae* (Dean et al. 2012). AvrPiz-t is an effector encoded by *M. oryzae* that is secreted into the cytoplasm of rice cells and perceived by the NLR Piz-t to induce effector-triggered immunity (ETI) (Luo et al. 2004; Li et al. 2009; Park et al. 2012). Solution structure of AvrPiz-t has been determined, showing that it is a globular protein composed of six β strands and several loops (Zhang et al. 2013). A screen of AvrPiz-t interaction protein (APIP) with yeast two-hybrid (Y2H) method in a rice cDNA library identified 12 protein candidates, named APIP1–APIP12 (Park et al. 2012). The first studied APIP was APIP6, a RING-type E3 ligase that is important for pathogen-associated molecular pattern (PAMP)-triggered immunity (PTI) against *M. oryzae* of rice (Park et al. 2012). AvrPiz-t interacts with APIP6 and inhibits ubiquitin ligase activity of the latter, thereby suppresses PTI of rice (Park et al. 2012). Later, studies were conducted on other APIPs. APIP4, a trypsin inhibitor, could interact with AvrPiz-t and Piz-t, and contributes to rice immunity to *M. oryzae* (Zhang et al. 2020). APIP5, a bZIP transcription factor, uses its N-terminal to interact with AvrPiz-t and Piz-t, which is important to suppress effector triggered necrosis (ETN) of rice (Wang et al. 2016). APIP10, also a RING-type E3 ligase whose activity can be inhibited by AvrPiz-t, can interact with transcription factors OsVOZ1 and OsVOZ2, both of which interact with Piz-t (Park et al. 2016; Wang et al. 2021). APIP12, a homologue of nucleoporin protein Nup98, could interact with AvrPiz-t and APIP6 with its different regions, and is involved in the rice basal resistance against *M. oryzae* (Tang et al. 2017). Therefore, we can see that of these APIPs, APIP6 and APIP12 do not interact with Piz-t, and are involved in PTI; APIP4 and APIP5 directly interact with Piz-t, while APIP10 indirectly interact with Piz-t, and the three APIPs are involved in ETI or ETN.

Besides performing its function through AvrPiz-t, APIP6 also interacts with OsELF3-2 (an orthologue of the *Arabidopsis* flowering and circadian regulator) and OsCATC (a catalase) and then degrades them, thereby negatively regulates rice immune response against pathogens (Ning et al. 2015; You et al. 2022). Moreover, APIP6 could work with rice UBC26, an E2, to ubiquitinate AvrPiz-t in vitro (Liu et al. 2021). Considering the versatile roles of the E3 ligase APIP6, we set out to elucidate how APIP6 performs its function with methods of structural biology. We determined crystal structure of the RING domain of APIP6 (APIP6-RING), which exhibits a new dimerization mode compared with reported RING motif proteins. In addition, we constituted and verified a complex model of APIP6 with E2, and proposed a working model of APIP6 with E2, Ub, and AvrPiz-t, which could expand our understanding of the functional mechanism of APIP6.

Results

Determination of the APIP6-RING crystal structure

To understand the structural mechanism of APIP6 functioning, we set out to determine the crystal structure of APIP6. APIP6 is a protein of 439 residues (Fig. 1a). The conserved residues of RING motif ($CysX_2CysX_{9\text{-}39}Cys_{1\text{-}3}HisX_{2\text{-}3}Cys/HisX_2CysX_{4\text{-}48}CysX_2Cys$) is at its N-terminal (residues Cys35–Cys80), while no other conserved domain was predicted. The full-length recombinant APIP6 protein precipitated during expression and/or purification in both *Escherichia coli* and insect cell. We then designed several truncates of APIP6, and was able to obtain the recombinant protein of residues Val33–Asn92 (named APIP6-RING hereinafter) that is stable in vitro (Fig. 1a). The structure of APIP6-RING was determined to 1.78 angstroms (Å) (Table 1). Each asymmetry unit contains two protein molecules, exhibiting a homodimeric conformation with buried area of 1023.4 $Å^2$ (Fig. 1b). All the residues of APIP6-RING were built into the model, together with an additional aspartate residue encoded by sequence from the vector that was observed at the N-terminal of the protein.

APIP6-RING exists as an unprecedented homodimer

An APIP6-RING molecule consists of two β strands (β1: Thr51–Leu54; β2: Gly57–His61) and one α helix (Leu62–Lys73) (Fig. 1b). The two β strands further constitute one pair of β hairpin, which could stabilize the overall conformation of the protein. Additionally, β hairpins from two APIP6-RING molecules form an anti-parallel β sheet, and the plane of each protein constituted by β hairpin and α helix are parallel (please

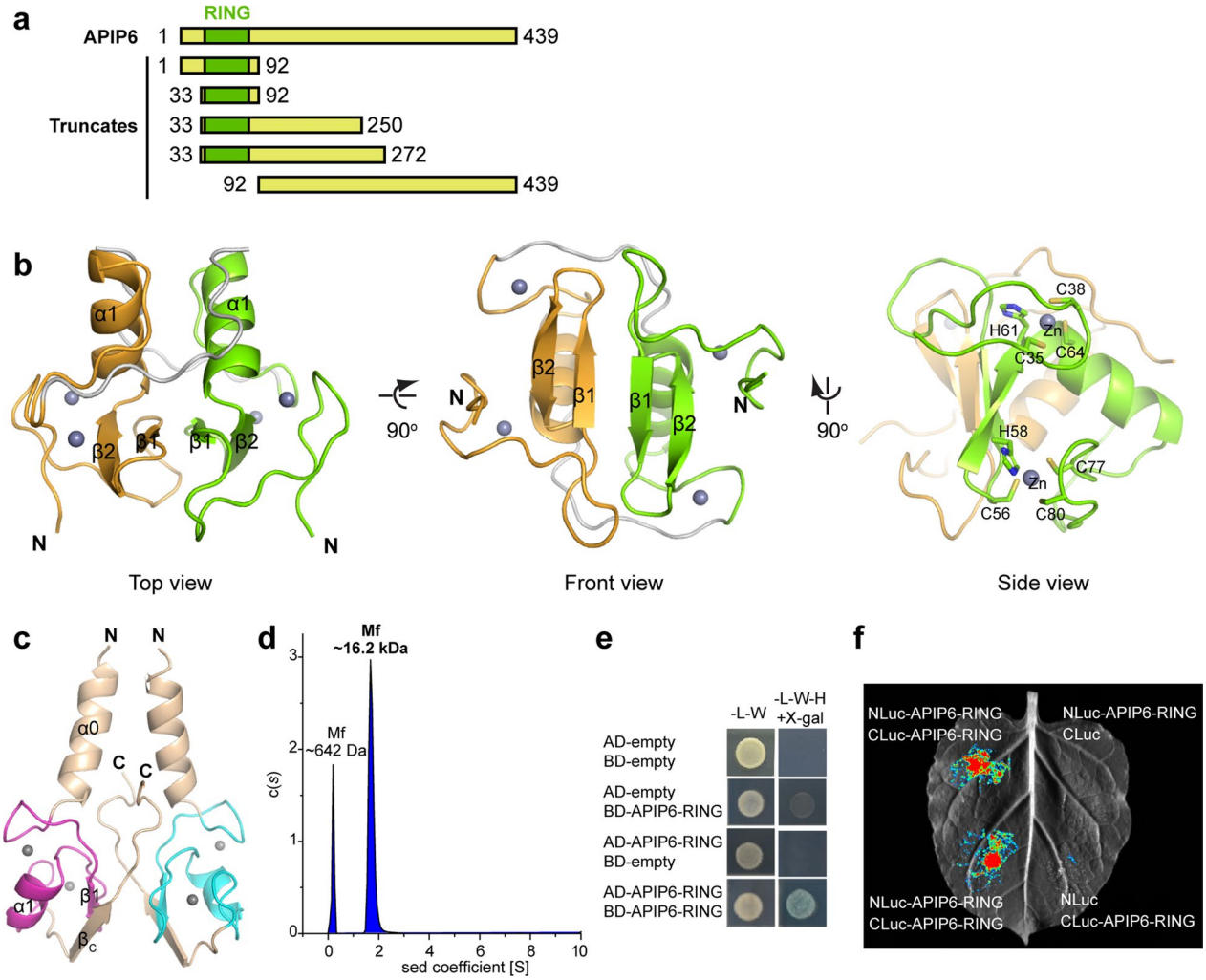

Fig. 1 Crystal structure of APIP6-RING exhibits a novel dimerization mode of RING-type E3s. **a** A diagram of APIP6 and its truncates. Protein crystal was only obtained with the 33–92 truncate. **b** Overall structure of the APIP6-RING homodimer. The two chains are colored chartreuse or light orange, respectively. The coordination residues to zinc ions are shown as sticks on the side view of the protein structure. **c** A representative homodimer of RING-type E3 (PDB accession number 2YHO), showing the dimer mode is different from APIP6-RING. The ring motif of the two molecules are colored pink and cyan, respectively, and the other regions are colored wheat. In **b, c**, zinc ions are shown as grey spheres. **d** Recombinant APIP6-RING protein mainly exists as homodimer in solution as evaluated by the SV-AUC method. Mf: calculated molecular weight of the corresponding fraction. **e** APIP6-RING protein forms homodimer as evaluated by Y2H assay. **f** APIP6-RING also forms dimer in vivo as shown by LCI assay

refer to front view of the homodimer), both of which likely render the dimer increased stability. Actually, the overall structure of APIP6-RING is almost centrosymmetric. Besides stable secondary-structural elements, each APIP6-RING molecule contains three loops: the long N-terminal loop (Val33–Ser50), the short β1–β2 loop (Gln55–Cys56), and the long C-terminal loop (Gly73–Ala91). Each protein contains two zinc ions, and the coordination mode of cysteine or histidine residues to zinc ions showed that APIP6-RING is a type H2 RING (Sun et al. 2019).

Homodimerization of RING-type E3s is frequent, but the dimer mode of APIP6-RING is unprecedented as compared with structures available in the protein data bank (PDB) (Fig. 1c and Additional file 1: Table S1). We evaluated whether the dimerization of APIP6-RING is an artifact resulted from crystal packing. Sedimentation velocity analytical ultracentrifugation (SV-AUC) assay determined the molecular weight of APIP6-RING in solution is 16.2 kDa, about two-fold of an APIP6-RING monomer (Fig. 1d). Y2H and firefly luciferase complementation imaging (LCI) assays showed that

Table 1 Diffraction data processing and structural refinement statistics of the APIP6-RING structure

Data collection and processing	
Beamline	SSRF BL19U1
Wavelength (Å)	0.9785
Space group	$P2_12_12_1$
Cell dimensions	
a, b, c (Å)	34.24 46.58 83.18
α, β, γ (°)	90 90 90
Resolution (Å)	40.64–1.78 (1.844–1.78)
Unique reflections[a]	13,316 (1294)
R_{merge}	0.072 (0.363)
$CC_{1/2}$	0.994 (0.988)
I/σ(I)	40.5 (3.78)
Completeness (%)	99.89 (99.92)
Redundancy	12.1 (9.3)
Refinement	
R_{work}	0.210
R_{free}	0.243
No. of non-hydrogen atoms	986
Protein	892
Ligand	4
Water	90
R.m.s.d	
Bond lengths (Å)	0.006
Bond angles (°)	0.85
Ramachandran plot (%)	
Favored	95.69
Allowed	4.31
Outliers	0.00
B-factors ($Å^2$)	
Average	45.24
Protein	44.97
Ligand	30.00
Water	48.50

[a] Values for the outer shell are given in parentheses

APIP6-RING interacts with itself in vivo (Fig. 1e, f). Therefore, APIP6-RING exists as a homodimer both in vitro and in vivo, and the dimer in the solved structure is not resulted from crystal packing.

Interactions between the two APIP6-RING molecules of the homodimer

Analyzing the interactions between the two APIP6-RING molecules, we found hydrogen bonds play a major role, whereas the contribution of hydrophobic interaction is trivial. In one homodimer, the two APIP6-RING molecules are nearly centrosymmetric, and thus most of the hydrogen bonds are symmetric (Fig. 2a, b). On the top of the front view of the homodimer, four pairs hydrogen bonds are formed between residues Arg53 and Gln55 of one chain and Ser50, Thr51, and Glu84 of the other chain; on the bottom of the front view, the other four pairs hydrogen bonds exist symmetrically to the former (Fig. 2a). On the left side of the back of the homodimer, residues Asp63, Ser67, and Asn70 form three pairs of hydrogen bonds with residues Leu89 and Asn87 of the other chain; on the right side, symmetric interactions exist (Fig. 2b). In addition, two pairs of hydrogen bonds are formed between the side-chain carboxyl groups of residues Asn70 of the two APIP6-RING chains (Fig. 2b). Besides, there are also unsymmetrical-intermolecular and water-mediated hydrogen bonds (Additional file 2: Figure S1). These hydrogen bonds render

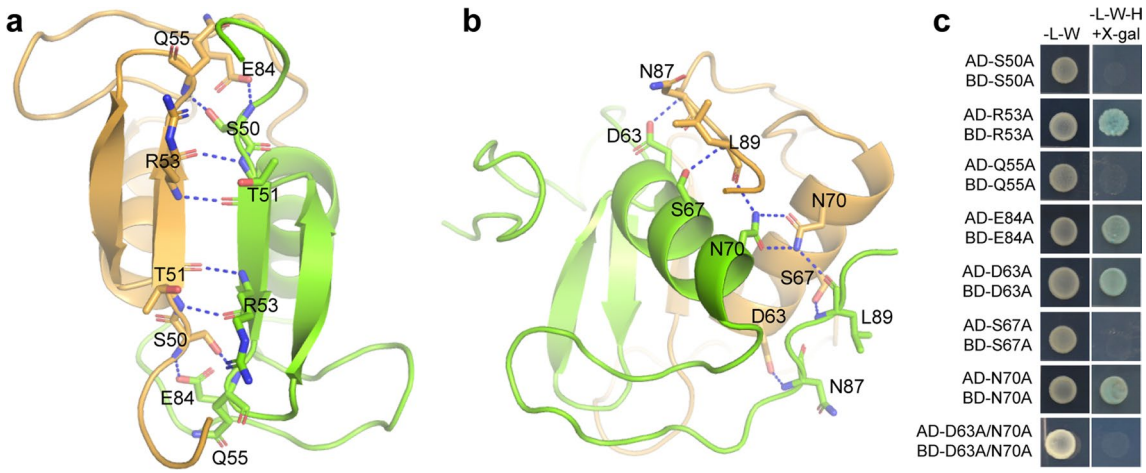

Fig. 2 Critical residues of APIP6-RING for its dimerization. **a** Residues of APIP6-RING that forms intermolecular hydrogen bonds as viewed from the front of APIP6-RING. **b** Residues of APIP6-RING that forms intermolecular hydrogen bonds as viewed from the back of APIP6-RING. In **a**, **b**, APIP6-RING model are viewed and colored as Fig. 1b, critical residues are shown as sticks, and hydrogen bonds are shown as blue dashed lines. **c** Verification of the critical residues of APIP6-RING for dimer formation with Y2H assay. Please find the control results in Additional file 2: Figure S2a

the APIP6-RING homodimer high stability with a ΔG of −4.5 kcal/mol as calculated with PISA of the CCP4 software suite (Potterton et al. 2003).

Evaluation of the critical residues for APIP6-RING dimer formation

We then designed mutational assays to evaluate the residues that contribute to intermolecular interactions. Single mutations of residues Ser50, Gln55, and Ser67 to alanine hampers dimer formation as evaluated with Y2H and LCI assays, suggesting intermolecular hydrogen bonds formed by these residues are critical (Figs. 2c, 3 and Additional file 2: Figure S2a). Residue Arg53 uses its main-chain to form hydrogen bonds with residue Thr51 of the other chain, and only Arg53 of one chain uses its side-chain amino group to interact with Ala44 of the other chain (one of the unsymmetrical-intermolecular hydrogen bond), thus mutation of Arg53 did not interrupt dimer formation (Fig. 2a, c and Additional file 2: Figure S1a). Side chains of residues Asp63, Glu84, and Asn70 participate in intermolecular interaction, but single mutation of them could not hamper dimer formation either, probably because the hydrogen bond energy contributed by them are not comparable to that of residues Ser50, Gln55, and Ser67 (Fig. 2a–c). We then carried out double mutation of residues Asp63 and Asn70, and the mutant was not able to form dimer, supporting our speculation above (Figs. 2c, 3). Meanwhile, the residues that prevented APIP6-RING dimer formation does not obviously influence the interaction between APIP6-RING and its corresponding E2 (we identified from rice, data not published) (Fig. 3).

Construction and verification of an APIP6-RING/E2 model

By analyzing the structures of RING-type E3s in complex with E2 or E2/Ub deposited in the PDB, we found the interaction mode between RING-type E3 and E2 is generally conserved. Therefore, we attempted to construct a model of APIP6-RING/E2 complex (Additional file 1: Table S2) (Buetow and Huang 2016). The AlphaFold2-predicted three-dimensional model of E2 was obtained from the UniProt database. We used the RNF4/UBCH5A/Ub ternary complex (PDB accession number 4AP4) as a reference model (Fig. 4a) (Plechanovova et al. 2012). By structurally superimposition of one APIP6-RING molecule with the RING of the ternary complex, we identified the relative position of E2 to APIP6-RING and constructed an APIP6-RING/E2 complex model (Fig. 4b).

As the dimerization mode of APIP6 is different from other RING-type E3s, the complex of APIP6-RING with E2 stretches in different orientation from others (Figs. 1b, c and 4a, b). There are four residues (Ser36, Asp40, Asn79, and Arg81) of APIP6-RING that might be involved in hydrogen bond interactions with residues Asn18, Arg19, Ser106, and Ser108 of E2 (Fig. 4c). In addition, another three residues (Ile37, Ala68, and Pro78) of APIP6-RING possibly participate in hydrophobic interaction with residues Met75, Pro109, and Ala110 of E2 (Fig. 4d). We then carried out single point mutations of residues Ser36, Asp40, Asn79, and Arg81 on APIP6 that possibly form hydrogen bonds with E2, and found these mutants did partially lost E2 binding ability as evaluated by Y2H, co-immunoprecipitation (co-IP), and LCI assays (Fig. 4e, f and Additional file 2: Figures S2b, S3). Of the

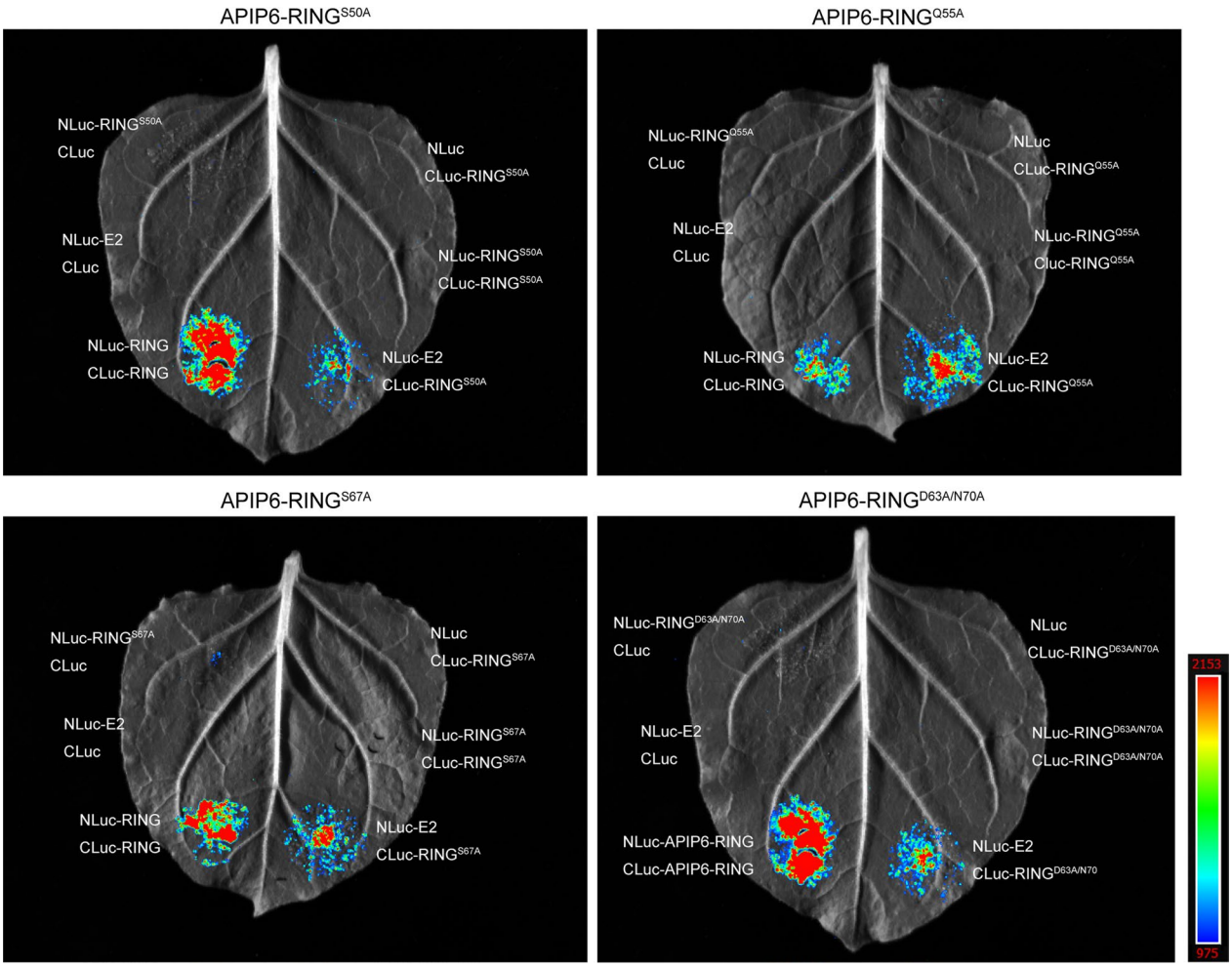

Fig. 3 Evaluation of the critical residues of APIP6-RING for homodimer formation with LCI assay. Only the four mutants, S50A, Q55A, S67A, and D53A/N70A that were proved to be critical for dimer formation with Y2H were further evaluated with LCI. Coding sequences of these mutants were cloned into vectors in-frame with NLuc and CLuc. E2 was cloned in-frame with NLuc and was used to evaluate whether these mutants hamper the interaction between APIP6-RING and E2

three residues of APIP6-RING that form intermolecular hydrophobic interactions with E2, only residue Ile37 possesses bulky side chain, and thus we mutated it to alanine (Fig. 4d). We found this mutant totally lost E2 binding ability, suggesting residue Ile37 plays a vital role in the interaction between APIP6 and E2 (Fig. 4e, f and Additional file 2: Figures S2b, S3). Collectively, these mutational studies showed that the APIP6-RING/E2 complex model is authentic.

Identification of the AvrPiz-t interaction region(s) on APIP6

APIP6 is a protein of 439 residues, but besides its N-terminal RING motif, no other conserved motif or domain was predicted, suggesting their function uncharacterized (Fig. 1a). In a ubiquitination process, E3 interacts with E2 and transfers ubiquitin conjugated to the latter to substrates. Therefore, there should be critical motif(s) on E3 that is responsible for substrate recognition and interaction. Since the RING motif is a well-acknowledged E2-interaction region, we wondered whether other regions of APIP6, i.e. the regions without conserved motif or domain, possess region(s) for interaction with AvrPiz-t, the substrate of APIP6. We then designed truncates of APIP6, and used Y2H to identify such region(s) on APIP6 (Fig. 5a and Additional file 2: Figure S2c). We found two regions, consisting of residues Pro120–Glu140 and Phe219–Gln254, respectively, are indispensable for AvrPiz-t interaction (Fig. 5a). Therefore, the C-terminal of APIP6 might works like a loop to interact with AvrPiz-t and then orient the latter to the ubiquitin on the APIP6/E2 complex.

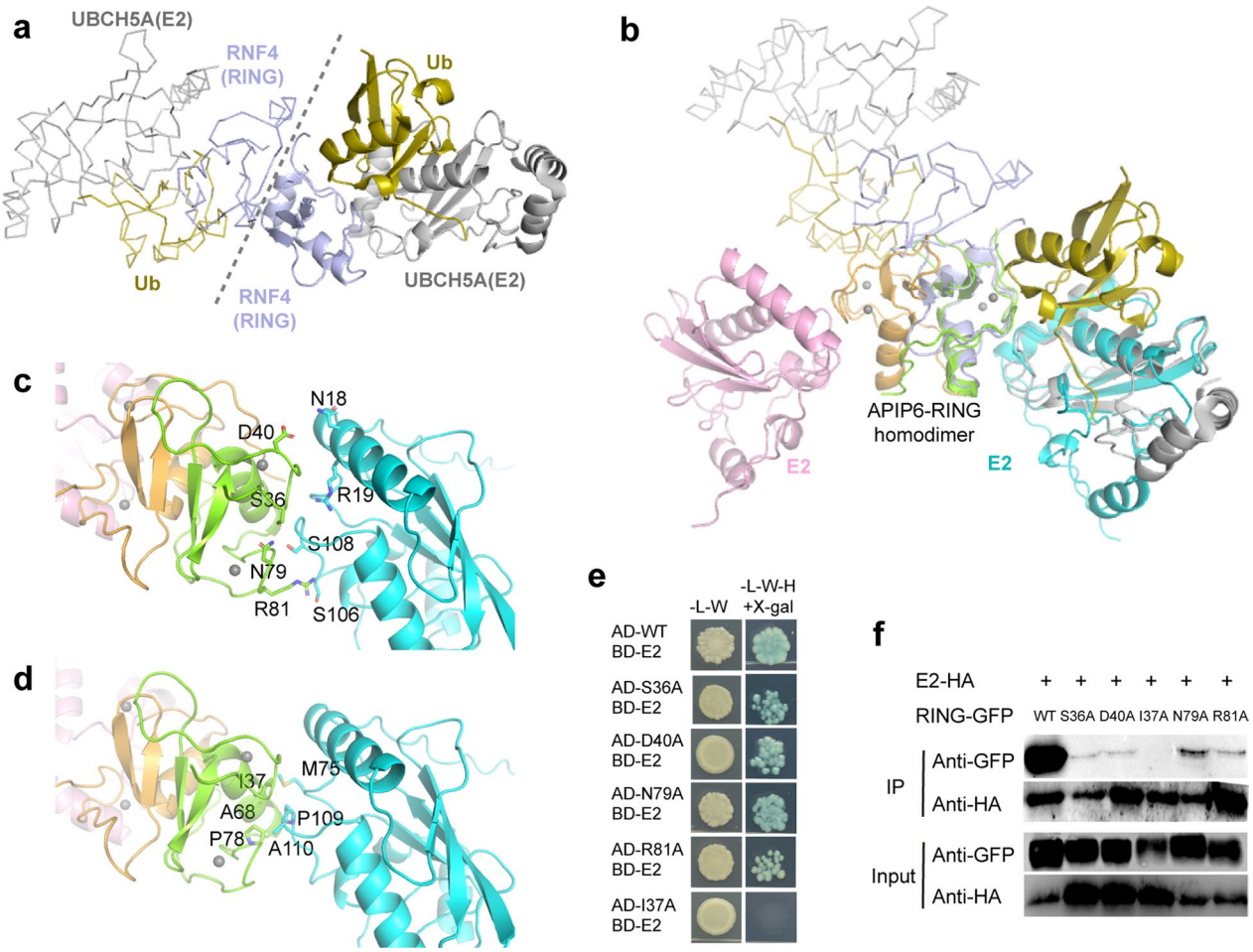

Fig. 4 An APIP6-RING/E2 complex model and its verification. **a** The RNF4/UBCH5A/Ub ternary complex structure (PDB accession number 4AP4) used for APIP6-RING/E2 model construction. This complex structure represents the conserved mode of E2/E3/Ub complex. The dashed line indicates the axis of symmetry. **b** The constructed APIP6-RING/E2 complex model based on the RNF4/UBCH5A/Ub complex. The RNF4/UBCH5A/Ub complex is shown as in **a**. **c** Residues of APIP6-RING and E2 that possibly form intramolecular hydrogen bonds. **d** Residues of APIP6-RING and E2 that possibly contribute to intramolecular-hydrophobic interactions. **e** Verification of the possible-critical residues with Y2H. **f** Verification of the possibly critical residues with co-IP

Discussion

Plants use various strategies to defend against the invasion of pathogens, a critical step of which is recognizing effectors or patterns from pathogens with cytosolic or cell-surface immune receptors (Ngou et al. 2022). AvrPiz-t is an avirulent effector encoded by *M. oryzae* that can elicit immune responses of rice (Luo et al. 2004; Li et al. 2009). Besides perceived by its corresponding NLR Piz-t through the mediation by APIP4, APIP5, and APIP10 to trigger ETI or ETN, AvrPiz-t can also be recognized by APIP6 as well as APIP12 to elicit PTI (Park et al. 2012, 2016; Wang et al. 2016; Tang et al. 2017; Zhang et al. 2020; Wang et al. 2021). As an E3 ligase, APIP6 also function on other proteins besides AvrPiz-t, rendering the elucidation of its detailed working mechanism more significance (Ning et al. 2015; Liu et al. 2021; You et al. 2022).

APIP6 is a protein of 439 residues, but only the N-terminal RING domain was predicted to have three-dimensional structural feature. We determined the crystal structure of APIP6-RING, and found it exists as an unprecedented homodimer. Typically, the β hairpins of two RING-type E3s interact in a 'face-to-face' mode (Fig. 1c). However, in the APIP6-RING structure, the β hairpins of two molecules interact in a novel 'shoulder-to-shoulder' mode (Fig. 1b). With a combination of several in vitro and in vivo assays, we confirmed that APIP6-RING does exists as a homodimer, and determined critical residues of APIP6 for its dimerization (Figs. 2, 3). Furthermore, we constituted and verified a

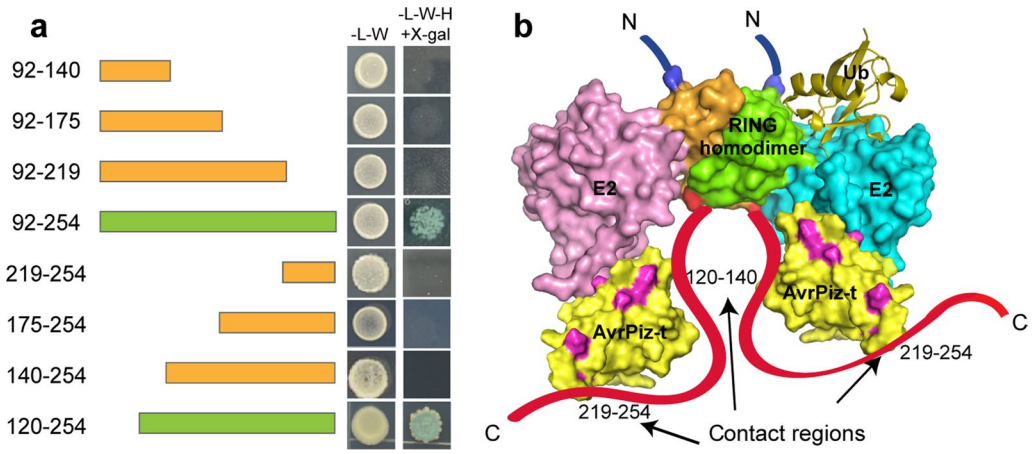

Fig. 5 Identification of AvrPiz-t interaction region(s) on APIP6 and a working model of APIP6. **a** Identification of the AvrPiz-t interaction region(s) on APIP6 with Y2H. Truncates of APIP6 were designed according to prediction of secondary structures. Truncates that could or could not interact with AvrPiz-t are colored green or orange, respectively. **b** A working model of APIP6 with ubiquitin-conjugated E2. The position of E2 and ubiquitin were determined by structural superimposition with the complex structure of RNF4/UBCH5A/Ub (PDB accession number 4AP4). The N-terminal and C-terminal regions of the RING motif of APIP6 are denoted as blue or red flexible lines. The two regions of APIP6, i.e. Pro120–Glu140 and Phe219–Gln254 that are responsible for AvrPiz-t interaction, are labeled. The determined solution structure of AvrPiz-t (PDB accession number 2LW6) was used to show the possible position of AvrPiz-t in the E2/APIP6/Ub complex model. The lysine residues on the surface of AvrPiz-t, which are probably to be conjugated to ubiquitin, are shown as pink

complex model of APIP6-RING/E2, and screened the region(s) of APIP6 for AvrPiz-t interaction (Fig. 5a).

According to the experimental results and analysis above, we are able to construct a working model of APIP6 (Fig. 5b). APIP6 uses its RING domain to form a homodimer, the mode of which is different from previously reported RING-type E3s. The RING domain interacts with E2, while the two regions (residues Pro120–Glu140 and Phe219–Gln254) of the C-terminal interact with the substrate AvrPiz-t, rendering lysine residues on the surface of AvrPiz-t more convenience for the acceptance of activated ubiquitin from E2 (Bai et al. 2019). The dimerization of the RING domain of APIP6 does not contribute to substrate interaction, but conformation of the dimer is likely more stable than monomer, providing a better platform for the sequential association of E2/Ub complex and substrate, and increasing the efficiency of ubiquitin transfer (Marianayagam et al. 2004). In this way, APIP6 synergizes with E2 to transfer ubiquitin to the substrate AvrPiz-t, thereby initiate the degradation of AvrPiz-t and induce the basal immune response of rice against *M. oryzae*.

Conclusion

By determination of its crystal structure, our research presents how APIP6 forms homodimer in a manner that has not been reported, how it preforms its function as an E3 ligase to mediate the interaction between E2/Ub and AvrPiz-t, and then elicit immune response of rice to counteract fungal pathogen.

Methods

Protein expression and purification

The *O. sativa* APIP6-RING (NCBI accession number XP_015640359.1, residues 33–91) was codon-optimized, cloned into the pHAT2 vector, and expressed in the *E. coli* BL21 (DE3) strain (Peranen et al. 1996). Single colony was inoculated into lysogeny broth (LB) medium supplemented with 100 μg/mL ampicillin and cultured with shaking (220 rpm) at 37°C. Induction of expression was performed by supplementation of 0.2 mM isopropyl-β-D-thiogalactopyranoside (IPTG) at an optical density at 600 nm (OD_{600}) of 0.6, and cultured for another 18 h at 18°C. Cells were collected with centrifugation and then resuspended in lysis buffer containing 20 mM Tris–HCl (pH 7.0), 500 mM NaCl, 20 mM imidazole, 2 mM DTT, and 100 μM $ZnCl_2$. After sonification, the suspension was centrifuged at 20,000 *g* for 20 min at 4°C. Recombinant protein was collected with nickel-charged resin and further purified with Superdex75 increase columns (Cytiva) equilibrated with buffer containing 20 mM Tris–HCl (pH 7.0), 300 mM NaCl, 2 mM DTT, and 5 μM $ZnCl_2$. All purification procedures were performed at 4°C or on ice.

Crystallization, data collection, and structure determination

The APIP6-RING recombinant protein was concentrated to 10 mg/mL for crystal screening with the sitting drop diffusion method at 18°C with the Oryx4 Instruments (Douglas). Crystals for data collection were grown with reservoir buffer containing 0.2 M NH_4F and 20% (v/v)

PEG 3350. For data collection, crystals were frozen in liquid nitrogen with reservoir buffer supplemented with 20% (v/v) glycerol.

Diffraction data were collected at the Shanghai Synchrotron Radiation Facility Beamline 19U1 (SSRF BL19U1). Data was indexed, integrated, and scaled with XDS (Kabsch 2010). Phase was obtained by molecular replacement with the structure of human RING-type E3 IDOL (PDB accession number 2YHO) using Phaser of the PHENIX software package, and optimized by iterative refinement with Refinement of the PHENIX and COOT (Emsley and Cowtan 2004; Adams et al. 2010; Zhang et al. 2011). Data processing and refinement result are listed in Table 1. All structural figures were made with PyMOL (DeLano 2002). Hydrogen bonds and hydrophobic contacts were determined using the CONTACT of the CCP4 software suite (Potterton et al. 2003).

Yeast two-hybrid (Y2H) assay

APIP6-RING (wild-type and mutants) were cloned into the pGBKT7 vector as bait or the pGADT7 vector as prey. E2 (GeneBank accession number ABG22107.1) was inserted into the pGBKT7 vector as bait. The prey and corresponding bait constructs were co-transformed into the *Saccharomyces cerevisiae* AH109 strain according to manufacturer's instructions. The transformants were cultured on SD-Leu/-Trp and SD-Leu/-Trp/-His plates at 30°C for 5 days for selection.

Sedimentation velocity analytical ultracentrifugation (SV-AUC)

APIP6-RING protein was exchanged to buffer containing 20 mM HEPES (pH 7.0), 500 mM NaCl, and 100 μM $ZnCl_2$. Prior to centrifugation, APIP6-RING was concentrated to OD_{280} of 0.8. Experiments were performed with an analytical ultra-centrifuge (ProteomeLab XL-I, Beckman Coulter, U.S.) at 226,000 *g* at 20°C. Absorbance data (λ = 280 nm) was acquired at time intervals of 300 s throughout the run. Data recorded from moving boundaries was analysed in terms of the continuous sedimentation coefficient distribution function *c*(*s*) using the program SEDFIT software (Brown and Schuck 2006).

Firefly luciferase complementation imaging (LCI) assay

The LCI experiment was carried out as described (Chen et al. 2008). Briefly, the vectors pCAMBIA1300-NLuc and pCAMBIA1300-CLuc contain the N-terminal luciferase (NLuc) fragment or the C-terminal luciferase (CLuc) fragment, respectively. APIP6-RING (wild-type and mutants) and E2 were cloned into the pCAMBIA1300-Cluc or pCAMBIA1300-nLUC vectors. *Agrobacterium* strain GV3101 transformed with plasmids carrying NLuc or CLuc were equally mixed and co-infiltrated into *Nicotiana benthamiana* leaves with a needleless syringe. The plants were kept in an illumination and humidity chamber at 25°C for 48 h. For observation of luciferase activity, infiltrated leaves were incubated with D-Luciferin potassium salt (substrate of luciferase) and measured with a luminometer.

Co-immunoprecipitation (co-IP) assay

APIP6-RING (wild-type and mutants) and E2 were cloned into the vectors pSUPER-GFP and pSUPER-HA, respectively. *Agrobacterium* strain EHA105 transformed with plasmids carrying GFP or HA tags were mixed and co-infiltrated into three-week-old *N. benthamiana* plants. After kept in an illumination and humidity chamber at 25°C for 48 h, proteins of *N. benthamiana* leaves were extracted and detected as described (Xu 2015). Total protein was captured with anti-GFP beads, and interaction between APIP6-RING (wild-type and mutants) and E2 were analyzed by immunoblotting with anti-GFP or anti-HA antibodies.

Abbreviations

APIP6	AvrPiz-t interacting protein 6
co-IP	Co-immunoprecipitation
E2	Ubiquitin conjugating enzyme
E3	Ubiquitin ligases
LCI	Luciferase complementation imaging
Luc	Luciferase
PDB	Protein data bank
RING	Really interesting new gene
SV-AUC	Sedimentation velocity analytical ultracentrifugation
Ub	Ubiquitin
Y2H	Yeast two-hybrid assay

Supplementary Information

The online version contains supplementary material available at https://doi.org/10.1186/s42483-023-00186-w.

Additional file 1: Table S1. Structures of RING-type E3 homodimers. **Table S2.** Structures of RING-type E3 in complex with E2 or E2/Ub.

Additional file 2: Figure S1. Other intermolecular hydrogen interactions in APIP6-RING homodimer. **Figure S2.** Controls of Y2H assays. **Figure S3.** Evaluation of the critical residues of APIP6-RING for E2 interaction with LCI assay.

Acknowledgements

We thank the staffs from BL19U1 beamline of National Facility for Protein Science (NFPS) at Shanghai Synchrotron Radiation Facility (SSRF) for their assistance during data collection.

Authors' contributions

JL and YN initiated the research; YZ, XZ, YL, JL, and DW designed the experiments; YZ, XZ, YL, TZ, and XW performed the experiments; XZ solved the structure; DW wrote the manuscript. All authors read and approved the final manuscript.

Funding

This work was supported by grant from the National Natural Science Foundation of China (Grant No. 32030089).

Availability of data and materials
The accession number for the APIP6-RING structure in the PDB is 8I3X.

Declarations

Ethics approval and consent to participate
Not applicable.

Consent for publication
Not applicable.

Competing interests
The authors declare that they have no competing interests.

Received: 14 February 2023 Accepted: 20 June 2023
Published online: 11 July 2023

References

Adams PD, Afonine PV, Bunkoczi G, Chen VB, Davis IW, Echols N, et al. PHENIX: a comprehensive Python-based system for macromolecular structure solution. Acta Crystallogr D Biol Crystallogr. 2010;66:213–21. https://doi.org/10.1107/S0907444909052925.

Bai P, Park CH, Shirsekar G, Songkumarn P, Bellizzi M, Wang GL. Role of lysine residues of the *Magnaporthe oryzae* effector AvrPiz-t in effector- and PAMP-triggered immunity. Mol Plant Pathol. 2019;20:599–608. https://doi.org/10.1111/mpp.12779.

Brown PH, Schuck P. Macromolecular size-and-shape distributions by sedimentation velocity analytical ultracentrifugation. Biophys J. 2006;90:4651–61. https://doi.org/10.1529/biophysj.

Buetow L, Huang DT. Structural insights into the catalysis and regulation of E3 ubiquitin ligases. Nat Rev Mol Cell Biol. 2016;17:626–42. https://doi.org/10.1038/nrm.2016.91.

Chen H, Zou Y, Shang Y, Lin H, Wang Y, Cai R, et al. Firefly luciferase complementation imaging assay for protein-protein interactions in plants. Plant Physiol. 2008;146:368–76. https://doi.org/10.1104/pp.107.111740.

Dean R, Van Kan JA, Pretorius ZA, Hammond-Kosack KE, Di Pietro A, Spanu PD, et al. The top 10 fungal pathogens in molecular plant pathology. Mol Plant Pathol. 2012;13:414–30. https://doi.org/10.1111/j.1364-3703.2011.00783.x.

DeLano WL. Pymol molecular graphics system. San Carlos: DeLano Scientific; 2002.

Emsley P, Cowtan K. Coot: model-building tools for molecular graphics. Acta Crystallogr D Biol Crystallogr. 2004;60:2126–32. https://doi.org/10.1107/S0907444904019158.

Kabsch W. Xds. Acta Crystallogr D Biol Crystallogr. 2010;66:125–32. https://doi.org/10.1107/S0907444909047337.

Li W, Wang BH, Wu J, Lu GD, Hu YJ, Zhang X, et al. The *Magnaporthe oryzae* avirulence gene AvrPiz-t encodes a predicted secreted protein that triggers the immunity in rice mediated by the blast resistance gene Piz-t. Mol Plant Microbe in. 2009;22:411–20. https://doi.org/10.1094/Mpmi-22-4-0411.

Liu X, Song L, Zhang H, Lin Y, Shen X, Guo J, et al. Rice ubiquitin-conjugating enzyme OsUBC26 is essential for immunity to the blast fungus *Magnaporthe oryzae*. Mol Plant Pathol. 2021;22:1613–23. https://doi.org/10.1111/mpp.13132.

Luo CX, Fujita Y, Yasuda N, Hirayae K, Nakajima T, Hayashi N, et al. Identification of *Magnaporthe oryzae* avirulence genes to three rice blast resistance genes. Plant Dis. 2004;88:265–70. https://doi.org/10.1094/PDIS.2004.88.3.265.

Marianayagam NJ, Sunde M, Matthews JM. The power of two: protein dimerization in biology. Trends Biochem Sci. 2004;29:618–25. https://doi.org/10.1016/j.tibs.2004.09.006.

Morreale FE, Walden H. Types of ubiquitin ligases. Cell. 2016;165:248-e1. https://doi.org/10.1016/j.cell.2016.03.003.

Ngou BPM, Ding PT, Jones JDG. Thirty years of resistance: zig–zag through the plant immune system. Plant Cell. 2022;34:1447–78. https://doi.org/10.1093/plcell/koac041.

Ning Y, Shi X, Wang R, Fan J, Park CH, Zhang C, et al. OsELF3-2, an ortholog of *Arabidopsis* ELF3, interacts with the E3 Ligase APIP6 and negatively regulates immunity against *Magnaporthe oryzae* in rice. Mol Plant. 2015;8:1679–82. https://doi.org/10.1016/j.molp.2015.08.004.

Park CH, Chen S, Shirsekar G, Zhou B, Khang CH, Songkumarn P, et al. The *Magnaporthe oryzae* effector AvrPiz-t targets the RING E3 ubiquitin ligase APIP6 to suppress pathogen-associated molecular pattern-triggered immunity in rice. Plant Cell. 2012;24:4748–62. https://doi.org/10.1105/tpc.112.105429.

Park CH, Shirsekar G, Bellizzi M, Chen S, Songkumarn P, Xie X, et al. The E3 ligase APIP10 connects the effector AvrPiz-t to the NLR receptor Piz-t in rice. Plos Pathog. 2016;12:e1005529. https://doi.org/10.1371/journal.ppat.1005529.

Peranen J, Rikkonen M, Hyvonen M, Kaariainen L. T7 vectors with a modified T7lac promoter for expression of proteins in *Escherichia coli*. Anal Biochem. 1996;236:371–3. https://doi.org/10.1006/abio.1996.0187.

Plechanovova A, Jaffray EG, Tatham MH, Naismith JH, Hay RT. Structure of a RING E3 ligase and ubiquitin-loaded E2 primed for catalysis. Nature. 2012;489:115–20. https://doi.org/10.1038/nature11376.

Potterton E, Briggs P, Turkenburg M, Dodson E. A graphical user interface to the CCP4 program suite. Acta Crystallogr D Biol Crystallogr. 2003;59:1131–7. https://doi.org/10.1107/s0907444903008126.

Pruneda JN, Littlefield PJ, Soss SE, Nordquist KA, Chazin WJ, Brzovic PS, et al. Structure of an E3:E2~Ub complex reveals an allosteric mechanism shared among RING/U-box ligases. Mol Cell. 2012;47:933–42. https://doi.org/10.1016/j.molcel.2012.07.001.

Soss SE, Klevit RE, Chazin WJ. Activation of UbcH5c~Ub is the result of a shift in interdomain motions of the conjugate bound to U-box E3 ligase E4B. Biochemistry. 2013;52:2991–9. https://doi.org/10.1021/bi3015949.

Sun J, Sun Y, Ahmed RI, Ren A, Xie AM. Research progress on plant RING-finger proteins. Genes. 2019;10:973. https://doi.org/10.3390/genes10120973.

Tang MZ, Ning YS, Shu XL, Dong B, Zhang HY, Wu DX, et al. The Nup98 homolog APIP12 targeted by the effector AvrPiz-t is involved in rice basal resistance against *Magnaporthe oryzae*. Rice. 2017;10:5. https://doi.org/10.1186/s12284-017-0144-7.

Vijaykumar S, Bugg CE, Cook WJ. Structure of Ubiquitin refined at 1.8 Å resolution. J Mol Biol. 1987;194:531–44. https://doi.org/10.1016/0022-2836(87)90679-6.

Wang R, Ning Y, Shi X, He F, Zhang C, Fan J, et al. Immunity to rice blast disease by suppression of effector-triggered necrosis. Curr Biol. 2016;26:2399–411. https://doi.org/10.1016/j.cub.2016.06.072.

Wang J, Wang R, Fang H, Zhang C, Zhang F, Hao Z, et al. Two VOZ transcription factors link an E3 ligase and an NLR immune receptor to modulate immunity in rice. Mol Plant. 2021;14:253–66. https://doi.org/10.1016/j.molp.2020.11.005.

Wang R, You X, Zhang C, Fang H, Wang M, Zhang F, et al. An ORFeome of rice E3 ubiquitin ligases for global analysis of the ubiquitination interactome. Genome Biol. 2022;23:154. https://doi.org/10.1186/s13059-022-02717-8.

Xu F, Copeland C, Li X. Protein immunoprecipitation using *Nicotiana benthamiana* transient expression system. Bio-protocol. 2015;5:e1520. https://doi.org/10.21769/BioProtoc.1520.

You X, Zhang F, Liu Z, Wang M, Xu X, He F, et al. Rice catalase OsCATC is degraded by E3 ligase APIP6 to negatively regulate immunity. Plant Physiol. 2022;190:1095–9. https://doi.org/10.1093/plphys/kiac317.

Zhang L, Fairall L, Goult BT, Calkin AC, Hong C, Millard CJ, et al. The IDOL–UBE2D complex mediates sterol-dependent degradation of the LDL receptor. Genes Dev. 2011;25:1262–74. https://doi.org/10.1101/gad.2056211.

Zhang ZM, Zhang X, Zhou ZR, Hu HY, Liu M, Zhou B, et al. Solution structure of the *Magnaporthe oryzae* avirulence protein AvrPiz-t. J Biomol NMR. 2013;55:219–23. https://doi.org/10.1007/s10858-012-9695-5.

Zhang C, Fang H, Shi X, He F, Wang R, Fan J, et al. A fungal effector and a rice NLR protein have antagonistic effects on a Bowman-Birk trypsin inhibitor. Plant Biotechnol J. 2020;18:2354–63. https://doi.org/10.1111/pbi.13400.